

Effective In-vehicle Intrusion Detection via Multi-view Statistical Graph Learning on CAN Messages

Kai Wang, Qiguang Jiang, Bailing Wang, Yongzheng Zhang, Yulei Wu

Abstract—As an important component of internet of vehicles (IoV), intelligent connected vehicles (ICVs) have to communicate with external networks frequently. In this case, the resource-constrained in-vehicle network (IVN) is facing a wide variety of complex and changing external cyber-attacks, especially the masquerade attack with high difficulty of detection while serious damaging effects that few counter measures can identify successfully. Moreover, only coarse-grained recognition can be achieved in current mainstream intrusion detection mechanisms, i.e., whether a whole data flow observation window contains attack labels rather than fine-grained recognition on every single data item within this window. In this paper, we propose StatGraph: an Effective Multi-view Statistical Graph Learning Intrusion Detection to implement the fine-grained intrusion detection. Specifically, StatGraph generates two statistical graphs, timing correlation graph (TCG) and coupling relationship graph (CRG), based on data streams. In given message observation windows, edge attributes in TCGs represent temporal correlation between different message IDs, while edge attributes in CRGs denote the neighbour relationship and contextual similarity. Besides, a lightweight shallow layered GCN network is trained based graph property of TCGs and CRGs, which can learn the universal laws of various patterns more effectively and further enhance the performance of detection. To address the problem of insufficient attack types in previous intrusion detection, we select two real in-vehicle CAN datasets that cover four new attacks never investigated before. Experimental result shows StatGraph improves both detection granularity and detection performance over state-of-the-art intrusion detection methods.

Index Terms—Controller Area Network, Intrusion Detection, Multi-view Statistical Graph, Graph-theory, In-vehicle Network.

I. INTRODUCTION

As an important part of vehicle-to-everything (V2X), intelligent connected vehicles (ICVs) equipped with in-vehicle communication networks and various embedded computing devices have begun to spread rapidly and become a popular trend [1]. Along with more and more intelligent

technologies integrated into vehicles, ICVs can obtain various intelligent services and comfortable experiences, including autonomous driving, collision avoidance, auto parking assist, and so on. However, these technologies also expose the in-vehicle network to attackers with more opportunities, and a large number of evolving new types of attacks have appeared in cyberspace, which threatens the security of in-vehicle network (IVN) and even the safety of passengers [2].

In terms of in-vehicle communication channels, Controller Area Network (CAN) technology is considered the de facto in-vehicle communication standard for Electronic Control Unit (ECU) in IVN embedded systems [3]. However, as a broadcast-like serial data communication protocol, CAN bus has a serious security vulnerability at its core mechanisms. Each CAN message contains only the priority determined by the message identifier and various control field information, but without mechanism for checking the identity of the sender, source address and destination address of the message. That leads to the opportunity for a large number of malicious messages such as digital level masquerade and data injection to be inserted to compromise the CAN bus in a vehicle. Once the malicious message overwrites the legitimate one, the attacker can control the associated operation. It can cause serious consequences if the malicious message involves the brake system, the powertrain, or the safety controls of the target vehicle [4].

With this in mind, recently researchers have chosen many methods to provide security of IVNs by detecting intrusion on CAN bus [5], [6], [7]. Encryption and authentication methods are effective for protecting IVNs [5], but it is generally necessary to add specific hardware to ensure the efficiency of encryption and decryption. As another security way, intrusion detection method does not require modification of the CAN protocol message fields and interactions, which has broader applicability for resource-constrained IVN environments [8].

As far as we know, the existing IVN intrusion detection gradually changes from detecting the physical characteristics of ECUs to detecting the CAN data flow characteristics of interactions between ECUs, and the more mainstream methods tend to use deep convolutional neural networks or recurrent neural network models, etc [6]. However, supervised neural network models mostly mark all the CAN messages within the whole data flow with attack labels no matter how many abnormal CAN messages it actually contains [9]. This results in the fact that only coarse-grained classification perfor-

This work was supported in part by the National Natural Science Foundation of China under Grant 62272129.

Wang Kai, Jiang Qiguang and Bailing Wang are with the School of Computer Science and Technology, Harbin Institute of Technology, Weihai, China. (e-mail: dr.wangkai@hit.edu.cn; jiangqiguang_971@163.com; wbl@hit.edu.cn)

Yongzheng Zhang is with the China Assets Cybersecurity Technology CO., Ltd. and Institute of Information Engineering, Chinese Academy of Sciences (CAS), China. (e-mail: zhangyz@cacts.cn)

Yulei Wu is with Faculty of Engineering and the Bristol Digital Futures Institute, University of Bristol, UK. (email: y.l.wu@bristol.ac.uk)

Kai Wang and Bailing Wang are the corresponding authors.

-mance can be achieved by existing intrusion detection methods, where only whether a whole message window anomaly or not can be identified, rather than every single message within this window. It not only weakens the detection granularity and accuracy, but also causes the problem of untraceability. Through research, many promising intrusion detection methods are excessive for the easily detectable attacks in current open dataset [10]. Besides, plenty of intrusion detections are from only a single-view perspective [11], which lack full feature extraction and utilization of ECU interaction data, resulting in low generalization ability.

To solve the above problems, we propose the Effective Multi-view Statistical Graph Learning Intrusion Detection (StatGraph) for IVN. StatGraph constructs the node feature vectors and adjacency matrixes for GCN by generating two statistical views, a timing correlation graph (TCG) and a coupling relationship graph (CRG). In order to extract short-term temporal relationships between neighboring messages, global features of input nodes are generated by designed statistical graph attributes of TCGs, whose edges represent temporal correlation between different CAN message IDs in given observation windows. Complementing complex correlations for node feature vectors gives the benefits of StatGraph, which implements intrusion detection by merging global features provided by TCGs and local features provided by data content. Besides, edge attributes in CRGs denote the neighbour and similar property in given message windows to enhance the association between the same IDs spanning the long-time axis. Thus, graph attributes extraction and utilization for two-views graphs have a vastly positive impacts on the training of a lightweight shallow layers GCN. In addition, since it is not feasible to verify the physical impact of simulated data on real vehicles, accompanied by insufficient detection of attack types by previous intrusion detection. We select two real in-vehicle datasets, Car Hacking Dataset and ROAD dataset, that cover five new attacks never investigated before. Experimental results show that StatGraph is able to accurately identify the masquerade attack that is undetectable before, with an average accuracy rate of over 99.4% and in very low 6.1% misclassification for denial of fabrication attack. The outstanding results on 2 kinds of datasets for simple attacks and masquerade attack verify the good generalization ability and robustness of StatGraph.

The main contributions of this paper are as follows:

1. We propose StatGraph to detection masquerade attack in fine-grained level by combining the message content with the statistical message graphs TCGs and CRGs in the form of a CAN message window, which improves detection performance by learning the universal rule in the various pattern via both short-time and long-time features.
2. We introduce a new criterion for granularity evaluation, Identification Granularity (IG), which is used to depict the recognition accuracy for each message at a fine-grained granularity rather than a whole window of messages at a coarse-granularity .
3. We select two real publicly available in-vehicle datasets: Car Hacking Dataset and ROAD dataset, to cover as many types of attacks as possible. In addition, we analyze 5 mas-

querade attacks, which are not seen in previous approaches and provide performance tests of the other four methods on ROAD dataset. We provide the prototype implementation¹ of StatGraph, whose experiment under above two different types of real CAN datasets validates the generalization ability and robustness of our method.

The remind of this paper is organized as follows: Section II summarizes existing CAN IDS methods. Section III introduces the CAN protocol and attacks on the CAN bus. Section IV describes our proposed StatGraph. In section V, experiment setup and results are shown. Section VI presents discuss and section VII concludes the paper.

II. RELATED WORK

It is urgent for intrusion detection to protect IVN environments from security threat. Most of the previous CAN intrusion detection approaches are based on deep learning, such as convolutional neural network (CNN) [9], Long Short Term Mermory network (LSTM) [12], via analyzing data fluctuations, regularity, information entropy and other features in the CAN bus. A deep convolutional neural network is used in [9] to learn data stream features for intrusion detection in CAN bus. In [13], an IDS based on voltage fingerprinting and CNN is designed that can detect attacks sent by the monitored ECU. The work in [12] used a typical LSTM structure and detected intrusions through anomaly analysis based on Time Series Prediction methods. However, as with previous deep learning-based approaches, the attacks contained in their dataset are unrealistically simplified and different from the actual complex network attacks, which leads to the impotency of these methods to cope with attacks.

On the other hand, due to the strict computational constraints of automotive ECUs, the resource-constrained IVN environment not suitable for application of linear stacked neural networks with high resource consumption. Note that our previous work has provided not only a quantitative and fair comparative performance analysis of deep learning-based intrusion detection methods for CAN bus, but also the lightweight intrusion detection method as a future improvement direction, see [6].

As distinct from deep learning methods, graph-based methods achieve intrusion detection via data distribution pattern of CAN bus. In [14], the authors proposed a CAN bus defense system based on graphs and chi-square tests, which has a stronger interpretability and a relatively simple operation method than deep learning-based methods. However, this method only relies on the statistical regularity reflected by the CAN periodicity and cannot implement accurate detection when the attack affects the periodicity. Moreover, considering the aspect of detection accuracy, detecting whether there is an injection attack in every 1200 CAN messages cannot reach the realtime requirement for IVN security and safety. Yet this method provides a graph-based intrusion detection idea. Graphs are a more complex data structure often used for modeling complex relationships. In contrast to CAN intrusion

¹The implementation of StatGraph and relevant datasets: <https://github.com/wangkai-tech23/StatGraph>

detection that analyzes context, graph theory-based methods are more suitable for learning features of data interactions between ECUs. As far as we know, there is a little CAN intrusion detection literature based on graph theory, which focus on processing only one graph [14], [15]. However, real-world graph data is much more complex, and it is often necessary to use multiple views to better represent real graph data, where each graph view commonly represents a kind of relationship between nodes. For example, in an ECU interaction network, one graph view may represent an ID association relationship, while another graph view may be a message timing relationship. Focusing on the collaborative process and data distribution pattern of the CAN bus reflected by the data interaction between ECUs drives us to propose an effective intrusion detection approach using graphical methods.

III. BACKGROUND

A. CAN Protocol

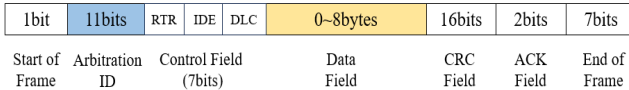


Fig. 1. CAN frame

CAN is a message-based communication standard that connects various ECUs in the vehicle and supports message passing between ECUs. The ECU is the electronic control unit of the vehicle and drives the vehicle's activities. The CAN bus enables the connection of various classic in-vehicle networks, including the OBD, infotainment system and various types of connected ECUs via gateways. Each ECU receives the CAN message and converts the bit sequence to extract the necessary components, such as arbitration ID, payload, remote transmission request (RTR).

In Figure 1, a standard CAN data frame describes these messages passed in the CAN bus. Each message mainly consists of several fields: CAN ID, data field, cyclic redundancy check (CRC) and RTR, etc. Therein, two fields are relevant to the scope of this paper: the 11-bit Arbitration ID and the 64-bit data field.

Typically, the **arbitration ID**, namely interchangeably referred to as **ID**, of a CAN message is used as a priority during the conflict between two or more CAN messages. The lower the ID is, the higher the priority keeps. The receiver decides whether to execute the CAN message or not according to the arbitration ID. This is used to resolve a conflict between CAN messages when multiple ECUs are transmitted. CAN ID not only determines its priority on the CAN bus, but also serve as an identifier for the message's contents. In general, each ECU is assigned a set of IDs that only given ECU can transmit. For example, the Power Control Module (PCM) may transmit messages with ID 0x102 and ID 0x45D, respectively. ID 0x102 contains signals for engine Revolutions Per Minute (RPM), vehicle speed and odometer every 0.05 s, and ID 0x45D contains signals for coded gas and brake pedal angle

every 0.01 s. A typical CAN setup for a vehicle will label each message with an ID and then transmit onto the CAN bus. An ECU master a subset of the message IDs seen in the network. Noted that CAN frames with the same ID encode the same set of signals in the same format and are usually sent to the transmitter at a fixed frequency to update the signal value.

The **DataField** (namely payload) contains up to 8 bytes of actual message content, which carries the data to be delivered.

In Figure 2, some sampled CAN messages frames sorted according to **timestamp** are given. Timestamp is the time point when each CAN message arrives at the collection device of CAN bus.

Timestamp:	0.131112	ID: 0220	000	DLC: 8	ee 03 f4 03 09 00 45 10
Timestamp:	0.131348	ID: 0260	000	DLC: 8	05 21 00 30 ff 93 63 02
Timestamp:	0.131584	ID: 02a0	000	DLC: 8	02 00 60 9d db 0c ba 02
Timestamp:	0.131817	ID: 0316	000	DLC: 8	05 22 a6 0a 21 1a 00 7f
Timestamp:	0.132049	ID: 0329	000	DLC: 8	40 a7 7f 8c 11 2f 00 10
Timestamp:	0.132291	ID: 0370	000	DLC: 8	ff 20 00 80 ff 00 00 a0
Timestamp:	0.132532	ID: 043f	000	DLC: 8	10 50 60 ff 4b 88 09 00
Timestamp:	0.132774	ID: 0440	000	DLC: 8	ff 00 00 00 ff 88 09 00
Timestamp:	0.133014	ID: 0545	000	DLC: 8	d8 0f 00 8a 3c 00 3c 00
Timestamp:	0.134759	ID: 04b0	000	DLC: 8	00 00 00 00 00 00 00 00
Timestamp:	0.134975	ID: 0164	000	DLC: 8	00 08 00 00 00 00 0e 06
Timestamp:	0.135422	ID: 02b0	000	DLC: 5	15 00 00 07 ed
Timestamp:	0.135656	ID: 0165	000	DLC: 8	0f e8 7f 00 00 00 0d 95

Fig. 2. some samples of CAN message

B. Compromised ECU

ECUs use bit-by-bit arbitration and explicit broadcasting to deliver CAN protocol messages, thus realizing fast and efficient data exchange. However, weak access control of communication interfaces, and lack of authentication of data interactions make vehicles vulnerable to malicious attacks. The adversary can physically access the CAN bus through the OBD-II port or control the telematics device by exploiting vehicle telematics service provided by the OEM. The authors in [10] provide a clearly defined attack model with widely used terms, which is useful to help understand attack sophistication:

1) **Weakly compromised ECU**: The adversary is capable of suspending any message transmission of a weakly compromised ECU node.

2) **Fully compromised ECU**: The adversary can totally control an ECU node, including sending forged messages and accessing the node's memory.

C. Messages injection attack

We introduce the following three general categories of attacks.

1) **Fabrication Attacks**: Use a fully compromised ECU to fabricate and inject malicious messages using forged IDs and Data Fields.

DoS Attack: The adversary injects massive messages with ID 0x000 and random payload to CAN bus. As ID 0x000 represents the highest priority, it always earns arbitration. These high-frequency and high-priority messages are sent by illegitimate ECUs, which results in flooding the CAN bus and preventing the vehicle from responding to legitimate CAN messages in a timely manner and physical impacts in

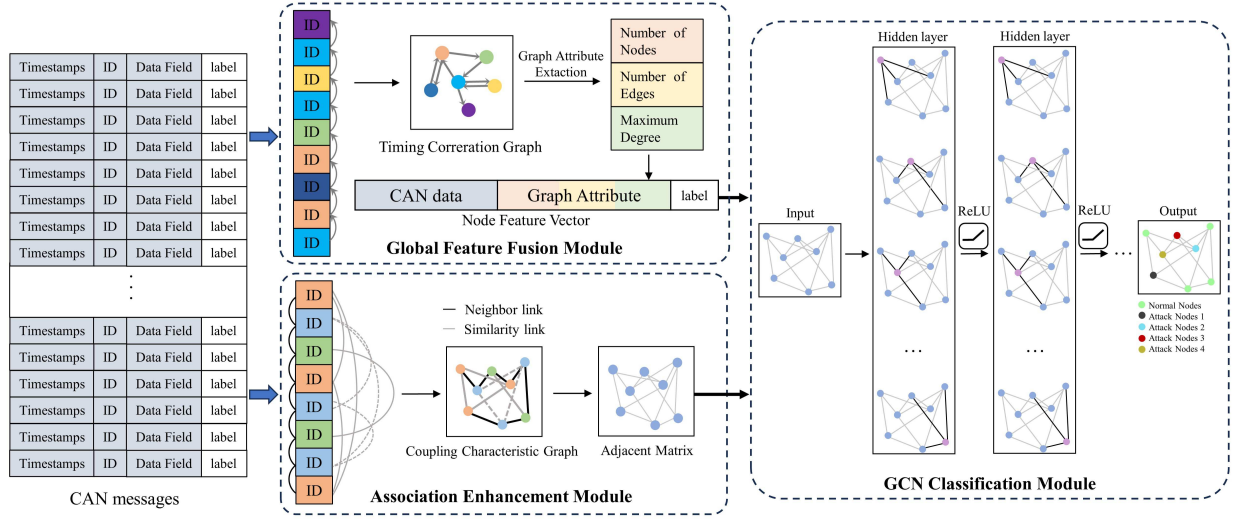


Fig. 3. The architecture of StatGraph

the vehicle such as intermittent steering control, intermittent acceleration control, flashing dashboard indicator light, etc.

Fuzzy Attack: Massive messages with random IDs and arbitrary payloads are injected, which causes bus flooding and interferes with the transmission of legitimate messages. The bus is taken over by injected messages instead of real messages, bringing similar physical behavior as the DoS attack. However, unlike DoS attack that delays legitimate CAN bus messages by occupying the CAN bus, since the injected messages may have IDs that appear in normal traffic, the receiver node reads and uses the information in the malicious payload, resulting in abnormal vehicle behavior.

targeted ID Attack: This attack is targeted to inject specific target ID and operational data field messages. The literature [16] described the characterize of fabrication attacks that is the inherent problem of *message confliction* in actuality. The problem with CAN messages caused by injection fabrication attacks is that an adversary can inject arbitrary messages onto the bus while legitimate ECUs are still sending legitimate messages. This leads to message conflicts. From the perspective of the receiving ECU, receivers have to decide what to do with this conflicting information after receiving inconsistent messages.

It is known from advanced reverse engineering signal processing techniques [16]: Generally, the ECU will consider the last seen data frame on a given ID. Therefore, in order to overwrite the legitimate message with the targeted ID, the injected frame must appear on the bus soon after the real frame. Two types of fabrication attacks, DoS and Fuzzy attacks, require little knowledge or observation of the target vehicle and are not incapable of performing fine-grained maneuvers. In order to successfully implement the targeted

ID attack, the adversary needs sniffing the CAN bus of the destination vehicle to explore the CAN bus messages that make the vehicle act unexpectedly. And it requires signal definitions based on a given ID designed as data fields with specific effects. In addition, targeted ID attacks can also be realized by flooding the bus, i.e., sending messages at a very high frequency, although this is easy to detect.

2) Suspension Attacks:

Launching the suspension attack, only needs a weakly compromised ECU. The adversary's purpose only needs to prevent the weakly compromised ECU from message transmission. This attack affects the performance of various other ECUs that utilize some information from weakly compromised ECU to function properly. As a result, suspension attacks can cause damage to not only weakly compromised ECU itself, but also other receiver ECUs.

3) Masquerade Attacks:

Masquerade attacks are the most complex class of attacks where the adversary needs to compromise two ECUs, one as a weakly compromised ECU and the other as a fully compromised ECU. The adversary first suspends a message with a specific ID from a weakly compromised targeted ECU, making the ECU unavailable. The fully compromised ECU is then used to transmit spoofed messages with given ID at the actual frequency, thus masquerading as the unavailable target ECU. Using this more advanced attack strategy, targeted ID attacks can be performed without message conflicts which allows more stealthy attacks. Evidently, launching masquerade attacks requires the prior knowledge or effort before the attack. And the target ECU under attacks can become out-of-order or can execute an adversary's command, which means more effort, more damage and higher risk.

IV. METHODOLOGY

As a representative intrusion detection method, the mainstream single-view graph-based intrusion detection specializes in exploring the relationship between the ID and frequency of CAN message data, but it may miss some masquerade attacks that only make changes to the payload field. For contrast, through our deep investigation, the combination of TCG-based graph attributes and payload from CAN message can successfully capture these anomalies because it combines global features within the window with local features at each node. Therefore, our proposed StatGraph introduces the TCG and CRG to enhance detection effectiveness which provides the multi-view perspectives for detecting intrusive attacks such as masquerade attacks.

A. System Overview

StatGraph can be divided into the following three main components: global feature fusion module, association enhancement module and GCN classification module, shown in Figure 3.

- Global feature fusion module can generate node feature vectors by extracting statistical graph attributes of built TCGs that describe CAN messages long-term distribution.
- Association enhancement module can produce adjacency matrixes by constructing CRGs whose edges reflect the interaction between CAN messages providing a novel view of correlation different from TCGs.
- GCN classification module can effectively fit the graph structure data from ECU interaction and perform a variety of classification tasks due to the assistance of the first two modules in improving the ability of the GCN model for classification.

After collecting the CAN message sequences and confirming observation windows, the global feature fusion module constructs TCGs through the timing correlation of ID pairs. We process the built TCGs that describe CAN messages long-term distribution for the purpose of generating node feature vectors with global feature by extracting statical graph attributes. Meanwhile, the association enhancement module builds CRGs through the short-time coupling relations of consecutive messages to generate adjacency matrixes, which can be processed in parallel with the global feature fusion modules. Then, we feed feature vectors and adjacency matrixes into GCN classification module for training and accomplishing classification task.

The StatGraph achieves effective and efficient IVN intrusion detection based on graph learning on the multivariate time series of CAN messages, which is defined formally as follows.

Definition 1: (Multivariate time series) CAN data is a multivariate time serie $\Psi \in \mathbb{R}^{T \times M}$:

$$\Psi = \{\psi_1, \psi_2, \dots, \psi_t, \dots, \psi_T\}, \quad (1)$$

where $\psi_t = \{timestamp, ID, d_1, \dots, d_8, label\} \in \mathbb{R}^M$. M is the dimension of a recorded data CAN message and we set $M = 11$ in this paper.

We extract an important part of the CAN bus protocol, the data field of CAN bus messages. And then transform them

from hexadecimal to decimal representation. Fill data whose length < 8 and then set the value of the data field as a vector $D = \{d_1, d_2, \dots, d_8\} \in \mathbb{R}^8$. Generally speaking, the length of data field should equal DLC, which has 3 different lengths: 2,5,8. If the length is not one of them, the fill value will be replaced by 255 instead of 0. Therefore, we display the information reserved for each CAN in the following form: $\phi_t = \{d_0, d_1, d_2, \dots, d_8, d_l\} \in \mathbb{R}^{10}$, where d_0 means CAN ID in decimal representation and d_l is label value that can indicate the type of attack.

Next, we define one term used in our proposed algorithm as:

Definition 2: A series of CAN messages monitored from the IVN CAN bus arranged according to the normal communication sequence can be regarded as located within a single observation window. In proposed algorithm, we consider N messages to be window size [14]. Let's assume that there are K windows in total. w_k denotes the matrix consisting of CAN messages within k -th window after preprocessing.

$$w_k = \{\phi_{k*N}, \phi_{k*N+1}, \phi_{k*N+2}, \dots, \phi_{k*N+N}\}. \quad (2)$$

Therein, $k \in \{1, 2, \dots, K\}$.

Definition 3: We consider two types of graphs, i.e., TCG $G(V, E)$ for long-term statical ID feature extraction and CRG $\hat{G}(\hat{V}, \hat{E})$ for short-term messages feature extraction, where $v_i, v_j \in V$ and $\hat{v}_i, \hat{v}_j \in \hat{V}$ denote the nodes; $e_{ij} \in E \subseteq V \times V$ and $\hat{e}_{ij} \in \hat{E} \subseteq \hat{V} \times \hat{V}$ represent the edges. Here, w_{ij} , \hat{w}_{ij} are the weight of edge e_{ij} and \hat{e}_{ij} respectively.

B. Global Feature Fusion Module

In this module, we design the TCG representing the CAN distribution over long-term to extract the interaction features of CAN data stream sequences. Because when an attacker performs attack operations such as injecting a large number of messages and modifying the frequency of sending ECUs, it may significantly affect the probability distribution of CAN messages. These relatively simple attacks CAN be efficiently detected by exploiting the statistical properties of TCGs that represent the long-term distribution of CAN.

• Generation of TCG based on CAN stream

Since the recurrent patterns of IDs are one of the manifestations of the periodicity for CAN messages. It is more precise and efficient to divide CAN messages into numerous windows and characterize the message distribution under each window separately. After dividing the CAN messages into K windows according to definition 2, our scheme designs Algorithm 1 to track legitimate transitions between the IDs of all two consecutive CAN messages and finally establish a TCG list, through multivariate time series CAN messages.

Specifically, for each N messages within a window, algorithm 1 treats each distinct CAN ID value as a node and constructs edges representing the ID-to-ID relationship. For convenience, $Set[ID_i] = \{\phi_n | \phi_n[d_0] = ID_i, \phi_n \in w_k\}$ denotes the set of messages whose ID value is the same as ID_i . A loop is iterated over all windows (Line 2). For the k -th window, different ID values are collected and a new ID key-value pair is created for the first occurrence of the ID value

in the window (Lines 4 and 8). Then we connect an edge to the ID value nodes corresponding to the two consecutive messages. If the edge already exists, the weight of the edge between the corresponding nodes will be increased (Line 11).

$$w_{i,j} \leftarrow \begin{cases} +1, & \phi_n \in \text{Set}[ID_j], \phi_{n+1} \in \text{Set}[ID_i], \\ +0, & \text{else.} \end{cases}$$

The algorithm keeps the graph G_k built by the current window (Line 14) and eventually returns the graphs G_1, \dots, G_K for all windows.

Algorithm 1 TCG Building Algorithm.

Input:

Observation Window List of CAN Messages:
 $CANWindowList = \{w_1, w_2, \dots, w_K\}$, therein
 $w_k = \{\phi_{k*N}, \phi_{k*N+1}, \phi_{k*N+2}, \dots, \phi_{k*N+N}\}$.

Output:

$CorrelationGraphList[G_1, G_2, \dots, G_K] \triangleright$ Timing Correlation Graph array of CAN bus data;

```

1:  $CorrelationGraphList \leftarrow []$ ,  $IDDictionary \leftarrow \{ " " : \}$ 
2: for  $w_k$  in  $CANWindowList$  do
3:   Initialize  $Graph$ ;
4:    $LastID \leftarrow \phi_{k*N}[d_0]$ ;
5:    $IDDictionary[LastID] \leftarrow len(IDDictionary) \triangleright$ 
   Create a new key/value pair in the dictionary;
6:   for  $i$  in  $N$  do
7:      $NowID \leftarrow \phi_{k*N+i}[d_0]$ ;
8:     if not  $NowID$  in  $IDDictionary.keys()$  then
9:        $IDDictionary[NowID] \leftarrow len(IDDictionary) \triangleright$ 
       Create a new key/value pair in the dictionary;
10:    end if
11:    Connect an edge from  $v_{IDDictionary[NowID]}$  to
     $v_{IDDictionary[LastID]} \triangleright$  Create link between two
    graph nodes;
12:     $LastID \leftarrow NowID$ ;
13:  end for
14:  Append  $Graph$  to the  $CorrelationGraphList$ ;
15:   $IDDictionary.clear \triangleright$  clear  $IDDictionary$ 
16: end for

```

- **Building feature vector of each node:**

After construction of TCG, graph feature vectors can be generated by statistical attributes of TCG, such as: the number of edges, the number of nodes, the max weight, the average weight, the max degree, etc. Our proposed method characterize feature vector for each CAN message, which could be defined as $X_{k,n}$, meaning node feature of n -th message in k -th window of raw CAN messages, $n \in \{1, 2, \dots, N\}$. Additionally, let X_k denotes node feature of k -th window, $k \in \{1, 2, \dots, K\}$.

Validated by extensive experiments, we choose extracting the node number, edge number, maximum degree from single constructed TCG and consider them as global features which will be supplemented to node feature vectors.

In addition, since some masquerade attacks may make changes to the payload field and ID. It is possible to more precisely detect masquerade attacks by merging the localized own payload of each CAN message information with the

global characteristics of the observation window in which the node is located. Hence, node feature $X_{k,n}$ is defined as $\{d_0, d_1, d_2, \dots, d_8, x_9, \dots, x_{11}\} \in \mathbb{R}^{12}$, where d_0 is CAN ID converted to decimal, d_1, d_2, \dots, d_8 means data value in data field and x_9, x_{10}, x_{11} represent node number, edge number, maximum degree of the TCG to which the node belongs, respectively. Furthermore, in order to ensure the detection granularity that can recognize each CAN message, the node feature $X_{k,n}$ retains each label indicating normal or injected, but it is not part of the input node feature vector.

C. Association Enhancement Module

In this module, we use CRG to enhance the association between the same IDs in short-term dependance. While TCG provides a perspective of the periodicity and statistical regularity of CAN messages, this is still not enough for accurate and efficient intrusion detection due to the constantly changing payload of legitimate messages with the same ID issued by ECUs.

The insertion of CRG reinforces the association of local features and assists in learning the common laws in CAN bus. However, the simplicity of the CAN message format has led many scholars to consider only contextual connections which are not sufficient in capturing CAN messaging associations mode. Since CAN messages are multivariate time series data, the short-term correlation of CAN messages is also a very significant feature when learning a new CAN message passing mechanism. In order to detect advanced masquerade attacks that only tamper with the content of CAN messages but not the ID, we need to more clearly fit the features of messages with various types of ID by enhancing the correlation between CAN messages with the same ID. This association between messages with the same ID can be referred to as content similarity and contextual relevance, also known as coupling relationships. Although much effort has been put into modeling graph structural information by existing techniques, they are limited in their ability to capture the perception of coupled relationships.

In this paper, coupling characteristic of data flow are reflected in the contextual correlation of two neighbour CAN message and the similarity of two CAN messages with the same CAN ID value. Consequently, a relationship-aware messaging paradigm is designed to reflect the coupling relationship and a new method is proposed to build adjacency matrix by establishing CRGs, shown in Algorithm 2.

From Definition 2, we set the same window as section IV-B. And we treat each CAN message in k -th observation window as a node to construct CRG with N nodes, whose edge represents the short-term relationship between messages. A loop is iterated over each window (Line 2). In k -th window, we define the nodes with the same ID value as a set $IDSet[ID_i] = \{\phi_n | \phi_n[d_0] = ID_i, \phi_n \in w_k\}$, which is constructed by counting the messages corresponding to each ID (Lines 5 and 9). Next, the algorithm constructs edges of CRG \hat{G}_k by searching coupling relationships. For i, j in

Algorithm 2 CRG Building Algorithm.

Input:

Observation Window List of CAN Messages:
 $CANWindowList = \{w_1, w_2, \dots, w_K\}$, therein
 $w_k = \{\phi_{k*N}, \phi_{k*N+1}, \phi_{k*N+2}, \dots, \phi_{k*N+N}\}$.

Output:

$RelationshipGraphList[\hat{G}_1, \hat{G}_2, \dots, \hat{G}_K] \triangleright$ Coupling
 Relationship Graph array of CAN bus data;

```

1:  $RelationshipGraphList \leftarrow []$ ,  $IDSet \leftarrow \{'' : \}$ 
2: for  $w_k$  in  $CANWindowList$  do
3:   Initialize  $Graph$ ;
4:    $LastID \leftarrow \phi_{k*N}[d_0]$ ;
5:    $IDSet[LastID] \leftarrow len(IDSet) \triangleright$  Create a new
   key/value pair in the dictionary;
6:   for  $i$  in  $N$  do
7:      $NowID \leftarrow \phi_{k*N+i}[d_0]$ ;
8:      $(\hat{v}_{i-1}, \hat{v}_i) \leftarrow 1 \triangleright$  Link two neighbor nodes (Context-
     tual correlation property);
9:     if not  $NowID$  in  $IDSet.keys()$  then
10:       $IDSet[NowID] \leftarrow [i] \triangleright$  Create a new key/value
      pair in the dictionary;
11:    else
12:      Append  $i$  to the  $IDSet[NowID]$ ;
13:      Link the edges between nodes in  $IDSet[NowID]$ 
       $\triangleright$  Connect all nodes with the same ID value
      (Similarity);
14:    end if
15:  end for
16:  Append  $Graph$  to the  $CorrelationGraphList$ ;
17:   $IDSet.clear \triangleright$  clear  $IDSet$ 
18: end for

```

$\{1, 2, \dots, N\}$, we have

$$\hat{e}_{ij} = \begin{cases} 1, & j = i + 1 \text{ or } i = j + 1, \\ 1, & \phi_j, \phi_i \in Set[ID_m], \\ 0, & \text{else.} \end{cases} \quad (3)$$

The first row in equation 3 indicates that an edge will be created between nodes corresponding to two consecutive CAN messages. (Line 7). The second row in equation 3 means that nodes with the same CAN ID value are connected to each other (Line 12).

Finally, algorithm 2 returns undirected graphs for multiple windows, i.e. CRGs, whose adjacency matrixes will be used to classification task in GCN via learning the universal rule in the various patterns.

D. GCN Classification Module

In this module, we built a multi-layer GCN model to identify and classify various attacks on the CAN bus by using training data that is converted into a graph structure by using methods provided by global feature fusion module and association enhancement module after exploring the relationship between each CAN bus message.

GCN [17] is a valuable approach for multi-classification on graph-structured data. Based on a first-order approximation of

graphs spectral convolutions, GCN model is able to encode both graph structure and node features in a valid way. And GCN achieves superior performance in various graph structure classifications by consistently merging node features in the graph. Therein, node feature vectors in graph neural network usually represent the node's own attributes or characteristics. On this foundation, this paper supplements the node feature vectors with the global recurrent rules brought about by the statistical graph properties of TCGs. The adjacency matrix is usually used to determine the message passing way of the graph neural network. Rather than being equally treated, aggregated messages of each node are weighted in a way using the adjacency matrix. It is important to choose the appropriate adjacency matrix to enhance the performance of the GCN, which is one of the reasons for the design of CRG.

Note that we use node classification of GCN to distinguish between its normal or injected attributes for each CAN message. This is the significance of keeping labels for each CAN message. The multi-layer GCN can be formulated as:

$$H^{(l+1)} = \sigma \left(\tilde{D}^{-1/2} \tilde{A} \tilde{D}^{-1/2} H^{(l)} W^{(l)} \right) \quad (4)$$

where $H^{(l)} \in \mathbb{R}^{N \times D}$ is the matrix of activations in the l -th layer, $W^{(l)}$ denotes the trainable weight matrix of l -th layer. $\sigma(\cdot)$ is the activation function. Denote number of hidden layer units as h , and $l \in \{0, 1, 2, \dots, L\}$. Set the adjacency matrix of the CRGs as A_k . $\tilde{A} = A_k + I_N$, I_N is the N dimensions identify matrix, \tilde{D} is degree matrix of \tilde{A} , $\tilde{D}_{ii} = \sum_j \tilde{A}_{ij}$. After multiple experiments, from the perspective of lightweighting and performance, our GCN model consists of an input layer, L hidden layers and a dense layer, shown in Table I.

TABLE I
STRUCTURE AND DIMENSIONS OF ALL LAYERS OF STATGRAPH.

Role	Layer Name	Data Shape	Activation	Dropout Ratio
Input	Input	$(B*N) \times 12$	-	-
	GCN 1	$(B*N) \times h$	ReLU	-
Feature Extraction	Dropout 1	$(B*N) \times h$	-	0.5
	GCN 2	$(B*N) \times h$	ReLU	-
	Dropout 2	$(B*N) \times h$	-	0.5
	GCN 3	$(B*N) \times h$	ReLU	-
	...			
	Dropout $l-1$	$(B*N) \times h$	-	0.5
	GCN l	$(B*N) \times h$	ReLU	-
	...			
	Dropout $L-1$	$(B*N) \times h$	-	0.5
	GCN L	$(B*N) \times h$	ReLU	-
Multi-classification	Dense	$(B*N) \times F$	Sigmoid	-

In order to improve the training efficiency of the model, we set $batchsize = B$, and the input $H^{(0)}$ is the continuous X_k splice of B . The last dense layer of GCN model returns $Z'_{k,n}$, where $Z'_{k,n} \in R^F | 0 \leq Z'_{k,n} \leq 1$. F is the number of classification categories. We consider output $Z'_{k,n}$ as the probability of $X_{k,n}$ being injected or which attack it is. The output of k -th window $Z_k = \{Z_{k,1}, \dots, Z_{k,N}\}$, where $Z_{k,n} \in \{0, 1, 2, \dots, F\}$ is employed to predict the attribute labels of the n -th message in the k -th window. In the training phase, the *cross-entropy* loss function compares real label of the n -th message in the k -th window to $Z_{k,n}$ through a sigmoid activation function.

In order to prevent overfitting, L2 regularization is used to restrict the values of weights. Besides, our GCN model is trained using the Adam optimizer, with a learning rate of 10^{-3} . In addition, we deploy *dropout* layers with a rate of 0.005 after each GraphConv layer. Moreover, we set the he rectified linear unit (ReLU), a widely used nonlinear function, as activation function in our model. It provides the neural network with nonlinear and allows neural network learning complex relationships in the data. And hyperparameters for training the StatGraph are shown in Table II.

TABLE II
HYPERPARAMETERS FOR TRAINING THE STATGRAPH MODEL.

<i>Hyperparameters</i>	Value(Car Hacking)	Value(ROAD)
B (Batchsize)	40	5
N (Window Size)	50	400
L (Total Number Of Layers)	4	1
h (Number of Hidden Layer Units)	32	32
F (Number of Categories)	5	6
Learning Rate	5×10^{-4}	5×10^{-4}
Weight Decay	5×10^{-4}	5×10^{-4}

This module makes full use of node features fusing statistical regulation represented by recurrent patterns of ID and adjacency matrices augmenting association relations for training, as a way to achieve high-performance fine-grained detection and classification of multiple attacks.

V. EXPERIMENT

In this section, comprehensive experiments are conducted to evaluate the performance of proposed StatGraph under fabrication attacks and masquerade attacks in CAN bus. In detail, first based on the proposed detection performance metrics at the fine-grained level, we compare StatGraph with anomaly detection baselines, in order to select *Window Size* for each method to achieve the best performance. Then the classification performance of each method is evaluated under the optimal window of various attacks.

A. Environment

In the experiments, the computer configuration is a 64 bit Inter(R) Core(TM) i7-13700 CPU @ 3.6GHz and a Geforce RTX 4080 32 GB GPU. PyTorch version 1.13 and Python 3.8 was used for train and test our StatGraph model.

B. Evaluation metrics

To evaluate the effectiveness of different methods, this paper used classic classification metric method. Accuracy, Precision and Recall can be calculated by using the number of true negatives (TN), true positives (TP), false negatives (FN) and false positives (FP), defined as follow:

$$\text{Accuracy} = \frac{TP + TN}{TP + TN + FP + FN} \quad (5)$$

$$\text{Precision} = \frac{TP}{TP + FP} \quad (6)$$

$$\text{Recall} = \frac{TP}{TP + FN} \quad (7)$$

Besides, F1-score is more useful than accuracy in the case of unbalanced class distribution. It is the harmonic mean of precision and recall, calculated as follow:

$$\text{F1-score} = \frac{2 \times \text{Precision} \times \text{Recall}}{\text{Precision} + \text{Recall}} \quad (8)$$

Identification Granularity (IG) is designed to evaluate the identification accuracy of intrusion detection methods at a fine-grained level. Based on the correct identification of the window (that is, the label of the k -th window, $label_k =$ the predicted value of the k -th window, $predict_k$), IG is calculated through TI (True Identification), which represents the number of correctly identified samples per window. Hence, The IG is defined as follows:

$$\text{IG} = \frac{1}{N} \sum_{k=1}^K \text{TI}_k \times C_k, \quad (9)$$

where

$$C_k = \begin{cases} 1, & label_k = predict_k, \\ 0, & label_k \neq predict_k. \end{cases}$$

C. Compared Methods

To compare with proposed StatGraph, we select a fast and efficient Chi-square statistical method and three excellent convolutional neural network models: EfficientNet, MobileNetV3, and CANet.

(1) Chi-square detection method [14]: Set the degrees of freedom to 5. Chi-square detection method is used on two population window: attack-free graph population and testing graph population, to recognize whether there is any attack happening or not.

(2) EfficientNet [23]: EfficientNet is a simple and efficient high-performance convolutional neural network after carefully balancing depth, width, and resolution. EfficientNet used a simple and efficient composite scaling method that allows us to easily scale the baseline ConvNet arbitrarily in a more principled way while satisfying resource constraints.

(3) MobileNetV3 [24]: MobileNetV3 combines the depth-wise separable convolutions of MobileNetV1, the inverted residual with linear bottleneck of MobileNetV2, lightweight attention model and using h-swish instead of swish function. This makes it is faster in computation and more friendly to quantization.

(4) CANet [25]: CANet consists of a two-branch dense comparison module which performs multi-level feature comparison between the support image and the query image. Introducing an attention mechanism makes effectively fuse information from multiple support examples under the setting of k-shot learning.

D. Dataset and Experimental Setup

To our best knowledge, there are currently existing seven public CAN datasets with labeled attacks (see Table III). From these, we select the ones that have real attacks on real vehicles. since simulated data may not always be legitimate in real vehicles. Specifically, as the most widely used dataset

TABLE III
OPEN CAN DATASETS.

Dataset	Real/Synthetic	attack		
		Fabrication	Suspension	Masquerade
CAN Intrusion Dataset(OTIDS) [18]	Real	Real;Dos;Fuzzing	-	-
Survival Analysis Dataset [19]	Real	Real;Dos;Fuzzing; targeted ID	-	-
Car Hacking Dataset [9] [20]	Real	Real;Dos;Fuzzing; targeted ID	-	-
SynCAN Dataset [21]	Simulated	Simulated; targeted ID	Simulated	Simulated
Automotive CAN Bus Intrusion Dataset v2 [22]	Real	Simulated; targeted ID	Simulated	Simulated
Can Log Infector	Real	-	-	Provide 7 types codes to simulate
Real ORNL Automotive Dynamometer (ROAD) CAN Intrusion Dataset [10]	Real	Real;Fuzzing; targeted ID	-	Simulated

in CAN IDS literature, Car Hacking Dataset captures ample instances containing multiple fabrication attacks. On the other hand, the highest fidelity CAN dataset, i.e. ROAD dataset, not only contains plentiful masquerade attacks, but also verifies the physical effects of all captured attacks and data from real vehicles. Previous IDSs on real datasets are often limited to fabrication attacks and lack masquerade attacks. Therefore, in this paper, Car Hacking dataset and ROAD dataset are chosen for validation of the effectiveness of detection method. The following is a detailed description and experimental setup for each selected dataset:

Car Hacking Dataset

Hacking and Countermeasure Research Lab (HCRL) of Korea University has produced Car Hacking Dataset by recording CAN traffic through OBD-II port in a real vehicle [9]. The dataset includes one normal dataset and four different attack datasets: DoS, Fuzzy, spoofing GEAR and spoofing RPM. In order to ensure the integrity of the window, we group the data within the entire window into one particular category. It is worth noting that we still keep its own label for each CAN frame. That is, the attacked window containing both the injected malicious frame and the normal frame is allowed.

For windows in normal dataset, we divide the data windows into training set and validation set with the percentages of 80%, 20%, respectively. And we use 70%, 20%, 10% of attack data windows for training, validation and test. And all normal windows in attack datasets are used to test. The dataset partitioned in this way has a large imbalance, which is closer to the situation in a real CAN bus when under attack. By the way, partition of dataset is the same, when using other models to perform training, validation and test.

ROAD Dataset

ROAD dataset [10] is collected from a passenger vehicle with a variety of CAN attacks, which contains the following seven advanced masquerade attacks:

1. Accelerator Attack (In Drive): It's a vulnerability-based attack without injection. The physical manifestation is a discrepancy between the vehicle's actions and the driver's operations: Regardless of the position of the gas pedal, acceleration occurs when the vehicle go into active gear.

2. Accelerator Attack (In Reverse): It's a vulnerability-based

attack without injection. The physical performance is that the vehicle accelerates to a fixed speed and maintains that speed regardless of the position of the gas pedal. When the brakes are released, the vehicle begins to accelerate.

3. Correlated Signal Attack Masquerade Attack: Each single ID transmitting four wheel speeds is injected with four dummy wheel speed values, all of which are quite different. If the speed of the frame injection is greater than or equal to the ambient frame, the effect is loss of throttle control of the vehicle. This loss of control begins immediately and continues throughout the injection period.

4. Max Engine Coolant Temp Masquerade Attack: Modifying the engine coolant signal value to the maximum(0xFF) causes light on the dash illuminates of engine coolant too high.

5. Max Speedometer Masquerade Attack: Modifying the speedometer signal value to the maximum(0xFF) causes speedometer to incorrectly display a maximum value.

6. Reverse Light Off Masquerade Attack: Modifying the reverse lights (off) value to on and keeping the car in Drive. This attack causes reverse lights cannot reflect which gear the car is in.

7. Reverse Light On Masquerade Attack: Modifying the reverse lights (on) value to off and keeping the car in Reverse. This attack causes reverse lights cannot reflect the gear of the car.

Note that ROAD dataset provides signals with labels translated using CAN-D algorithm [26] and raw data without labels. Because original equipment manufacturers (OEMs) of passenger vehicles hold secret their proprietary encodings of signals in the CAN data fields and vary the encodings across models. Besides, CAN-D algorithm is not 100% credible for unknown CAN signal translation. Signal translation method involves only the payload and not CAN ID and timestamps.

Hence, we compare the ID and timestamps of translated signals (CSV files) with those of raw data (log files), and consider the message with the same ID and timestamps value as one message, writing it into the same format like Car Hacking Dataset.

On this foundation, no message is labeled as an attack in accelerator attack drive dataset and accelerator attack reverse

TABLE IV
TEST RESULTS OF EACH METHOD IN MIX ATTACKS
(REAL-TIME DETECTION: $N = 3$, SEMI-REAL-TIME DETECTION: $N = 27$ AND OFFLINE DETECTION: $N = 54$).

<i>Method</i>	Window Size	F1-Score (Car Hacking)	IG (Car Hacking)	F1-Score (ROAD)	IG (ROAD)
EfficientNet	$N = 54$	0.1018	<u>0.0128</u>	0.3208	0.4664
	$N = 27$	<u>0.1382</u>	0.0054	0.3348	0.4957
	$N = 3$	0.1215	0.0041	<u>0.5236</u>	<u>0.9811</u>
MobileNetV3	$N = 54$	0.1018	0.0046	0.2861	0.4674
	$N = 27$	0.1109	0.0055	0.3411	0.4957
	$N = 3$	<u>0.1698</u>	<u>0.2815</u>	<u>0.6084</u>	<u>0.9285</u>
CANet	$N = 54$	<u>0.7347</u>	<u>0.8996</u>	0.1060	0.4664
	$N = 27$	0.5755	0.7910	0.1100	0.4942
	$N = 3$	0.7023	0.7229	<u>0.3585</u>	<u>0.9261</u>
StatGraph	$N = 54$	0.9403	0.9970	0.5763	0.9853
	$N = 27$	0.9403	0.9970	0.5763	0.9853
	$N = 3$	0.9403	0.9970	0.5763	0.9853

dataset. We discard these two attacks and select the remaining five attacks.

Except for the *max engine coolant temp masquerade attack* dataset, there are three files for the remaining attack data, whose three files are categorized into training, validation and test respectively. Besides, *max engine coolant temp masquerade attack* is divided into training set, validation set and test set according to 70%, 20%, 10% in window level.

E. Toward Real-time Detection

Notably, previous work labeled an entire segment of consecutive CAN messages containing at least one injection attack as an attack sample. An entire segment of consecutive CAN messages without an injection attack was labeled as a normal sample. However, there is no scientific explanation for the amount of data counted as an sample in previous researches. We give the selection criteria for the number of data by considering the speed of CAN bus sending messages and the latency specification in Intelligent Connected Vehicle and Industrial Control Internet.

To the best of our knowledge, the react time for the driver performing a braking action is 0.7 to 1.5 seconds [27]. Industrial automation control and remote driving require latency less than 10 ms. CAN has 125Kbps-1Mbps high speed, while the maximum length of CAN extended frame is 150 bit. After calculation, we can learn that the CAN bus sends 8 messages every 10ms at the minimum rate and 34 messages every 10ms at an average rate of 500kb/s. Hence, based on the two values 8 and 34, we set three intervals of Identification Granularity, $0 \sim 8$, $8 \sim 34$, $34 \sim +\infty$, to denote real-time detection, semi-real-time detection and offline detection, respectively. Hence, we choose the size of data window as 3, 27 and 54 respectively. The method of this paper is compared with previous methods in terms of F1-Score and IG on the three experimental scopes, and the performance is shown in Table IV. It is worth noting that the detection granularity of StatGraph is per message regardless of the window size N setting, so the results of the model with $N = 3$, 27, 54 of StatGraph are the same.

F. Detection performance

From Table IV, it can be observed that the StatGraph performs best on both CAN datasets. In order to further verify the effectiveness of our method, we choose the window size N corresponding to the optimal performance of each method for subsequent verification. (i.e. EfficientNet sets $N = 54$ for Car Hacking Dataset and $N = 3$ for ROAD dataset, MobileNetV3 sets $N = 3$ for both Car Hacking Dataset and ROAD dataset, CANet sets $N = 54$ for Car Hacking Dataset and $N = 3$ for ROAD dataset)

On this basis, Table V and Table VI show the Accuracy, Precision, Recall and F1-score of all the methods for various attacks on Car Hacking dataset and ROAD dataset, respectively. Since the chi-square detection method in [14] cannot set a consistent threshold for all multiple attacks, we only place the multi-classification detection results of compared neural network methods.

We observe that StatGraph has superior performance, with Car Hacking (0.9979) and ROAD (0.5763) achieving the highest F1-Scores. The experimental results demonstrated that StatGraph exhibited superior performance, which can correctly classify almost all CAN messages in Car Hacking Dataset of a fine-grained level and have best detection ability in ROAD dataset. One can also see that the generalizability of different models varies greatly. For example, EfficientNet and MobileNetV3 perform well on ROAD dataset but poorly on Car Hacking Dataset. While CANet has excellent performance on Car Hacking Dataset but works poorly on ROAD dataset. In contrast, StatGraph achieves highest F1-Score and IG values on both datasets.

In addition we present all the normalized confusion matrices on both two datasets in Figure 4 and Figure 5. In the Car Hacking Dataset, it is obvious that CANet and StatGraph have the highest degree of recognition for each classification. In the ROAD Dataset, the other three neural network models cannot identify reverse light off masquerade attack correctly, while StatGraph is able to identify some of these attacks.

G. Parameters Analysis

In this subsection, we research the effects of different parameters that can impact the performance of StatGraph to

TABLE V
TEST RESULTS OF EACH METHOD FOR DIFFERENT ATTACKS IN CAR HACKING DATASET.

Dataset	Attacks	Methods	Accuracy	Precision	Recall	F1-Score	Window Size/ Number of Identified Label
Car Hacking Dataset	DoS Attack	Chi-square	0.432	0.766	0.387	0.514	1200/1
		EfficientNet	0.0212	0.0474	0.998	0.0905	54/1
		MobileNet	0.2597	0.0675	0.9990	0.1265	3/1
		CANet	0.9005	0.1488	0.9891	0.2587	54/1
		StatGraph	0.9980	0.9953	0.9721	0.9836	1/1
	Fuzzy Attack	Chi-square	0.458	0.761	0.426	0.546	1200/1
		EfficientNet	0.0231	0.0328	1.000	0.0635	54/1
		MobileNet	0.2587	0.0227	0.9904	0.0443	3/1
		CANet	0.9007	0.2624	0.9867	0.4145	54/1
		StatGraph	0.9970	0.7804	0.8392	0.8088	1/1
	Drive GEAR Attack	Chi-square	0.608	0.721	0.594	0.651	1200/1
		EfficientNet	0.0288	0.0749	0.9991	0.1393	54/1
		MobileNet	0.2610	0.0833	0.9999	0.1537	3/1
		CANet	0.9013	0.9943	0.9937	0.994	54/1
		StatGraph	0.9980	0.9996	0.8920	0.9427	1/1
	RPM Attack	Chi-square	0.899	0.971	0.856	0.91	1200/1
		EfficientNet	0.0304	0.1077	0.9997	0.1944	54/1
		MobileNet	0.2623	0.0639	1.000	0.1202	3/1
		CANet	0.9015	0.8184	0.9935	0.8975	54/1
		StatGraph	0.9980	0.9932	0.9355	0.9635	1/1
Mixing Fabrication Attack	EfficientNet	0.0688	0.2526	0.8015	0.1018	54/1	
	MobileNet	0.081	0.255	0.804	0.111	3/1	
	CANet	0.9050	0.6447	0.9725	0.7347	54/1	
	StatGraph	0.9940	0.9275	0.9533	0.9403	1/1	

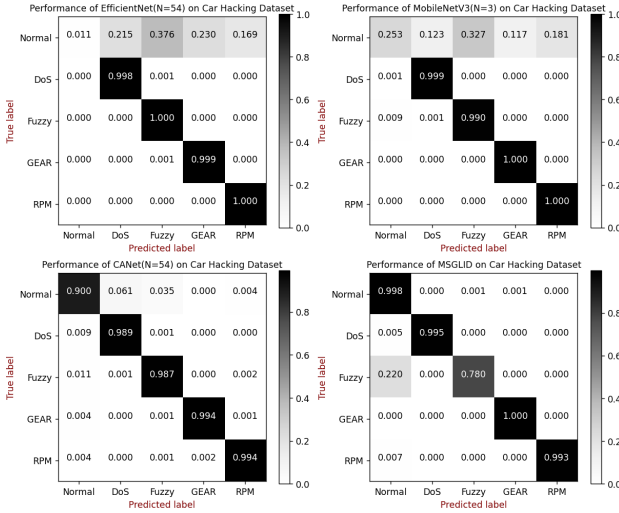


Fig. 4. Confusion Matrixes of Different Intrusion Detection Methods on Car Hacking Dataset.

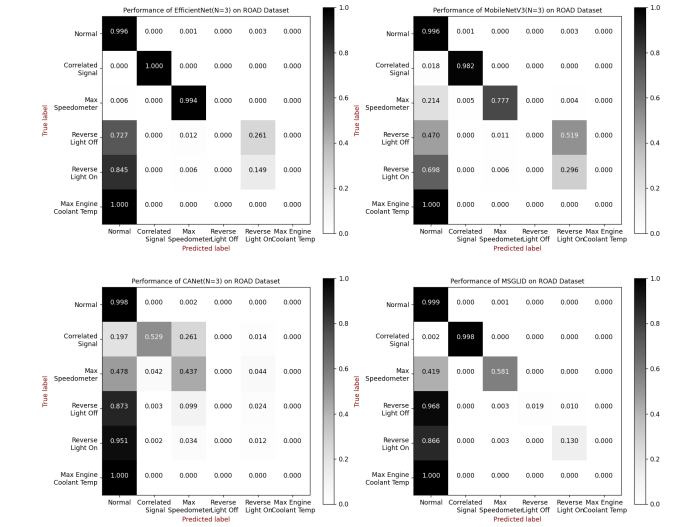


Fig. 5. Confusion Matrixes of Different Intrusion Detection Methods on ROAD dataset.

find the optimal window size N , number of hidden layers units h and batchsize B . The experiments are conducted as follows:

(1) Sensitivity to window size:

The performance comparison for different window sizes N is shown in Figure 6, ranging from 25 to 200 (Car Hacking) and 100 to 800 (ROAD). From Figure 6, it can be seen that the window size has a certain impact on the intrusion detection accuracy. If N is too large, one has to wait for more observations to detect intrusions. However, if N is too small, the informative contextual features cannot be adequately

incorporated. Relatively high F1-Score occurs with a window size $N = 50$ (Car Hacking), $N = 400$ (ROAD).

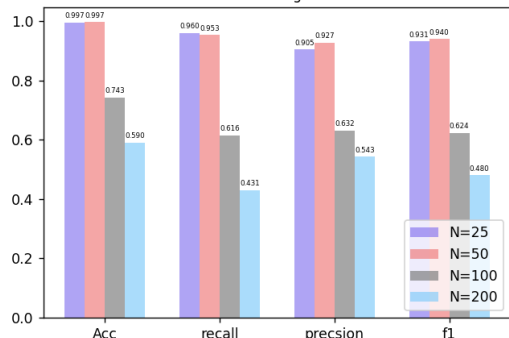
(2) Sensitivity to number of hidden layer units h :

Figure 7 illustrates the performance comparison in various dimensions of latent space. The dimensions of the latent space range from 16 to 64. We compare the results and find that using a large dimension of the latent space leads to a significant decrease in the F1 score. The reason for this may be that too large a dimension of the potential space can lead

TABLE VI
BEST TEST RESULTS OF EACH METHOD FOR DIFFERENT ATTACKS IN ROAD DATASET.

Dataset	Attacks	Methods	Accuracy	Precision	Recall	F1-Score	Window Size/ Number of Identified Label
ROAD Dataset	Correlated signal Masquerade Attack	Chi-square	0.540	0.450	0.818	0.581	1200/1
		EfficientNet	0.9960	0.9805	1.000	0.9902	3/1
		MobileNet	0.9949	0.9054	0.9054	0.9054	3/1
		CANet	0.9510	0.7108	0.5286	0.6062	3/1
		StatGraph	0.9990	0.9944	0.9976	0.9960	1/1
	Max Speedometer Masquerade Attack	Chi-square	0.625	0.143	0.556	0.227	1200/1
		EfficientNet	0.9960	0.9661	0.9937	0.9797	3/1
		MobileNet	0.9875	0.9825	0.7766	0.8675	3/1
		CANet	0.9240	0.7355	0.4368	0.5481	3/1
		StatGraph	0.9939	0.8839	0.5806	0.7008	1/1
	Reverse Light Off Masquerade Attack	Chi-square	0.603	0.448	0.591	0.510	1200/1
		EfficientNet	0.9848	0.0000	0.0000	0.0000	3/1
		MobileNet	0.9805	0.0000	0.0000	0.0000	3/1
		CANet	0.9403	0.0000	0.0000	0.0000	3/1
		StatGraph	0.9943	0.9787	0.0192	0.0377	1/1
	Reverse Light On Masquerade Attack	Chi-square	0.528	0.215	0.469	0.295	1200/1
		EfficientNet	0.9847	0.2457	0.1493	0.1858	3/1
		MobileNet	0.9854	0.2744	0.2965	0.2850	3/1
		CANet	0.9411	0.0665	0.0125	0.0210	3/1
		StatGraph	0.9950	0.8827	0.1299	0.2265	1/1
	Max Engine Coolant Temp Masquerade Attack	Chi-square	0.830	0.111	1.000	0.200	1200/1
		EfficientNet	0.9959	0.0000	0.0000	0.0000	3/1
		MobileNet	0.9956	0.0000	0.0000	0.0000	3/1
		CANet	0.9542	0.0000	0.0000	0.0000	3/1
		StatGraph	0.9990	0.0000	0.0000	0.0000	1/1
	Mixing Masquerade Attack	EfficientNet	0.9699	0.5281	0.5232	0.5236	3/1
		MobileNet	0.9637	0.5228	0.5084	0.5132	3/1
		CANet	0.9459	0.4111	0.3292	0.3585	3/1
StatGraph		0.9853	0.7876	0.4544	0.5763	1/1	

Performance of MSGLID on Car Hacking Dataset with $h = 32$ and $B = 40$



Performance of MSGLID on ROAD Dataset with $h = 32$ and $B = 5$

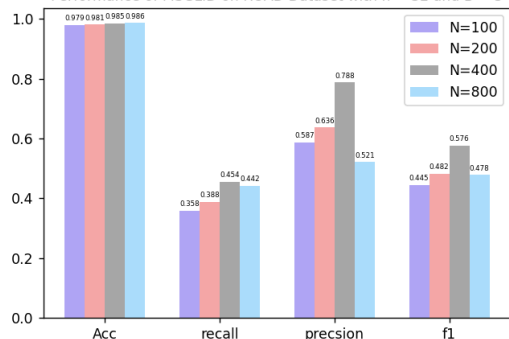


Fig. 6. Performance of StatGraph in Different Window Size N .

space can cause a large amount of information loss in the encoding stage making the GCN model poor performance. Hence, a suitable dimension 32 has outstanding results with the best F1-Score of both datasets, which makes StatGraph allow faster training and higher accuracy.

(3) Sensitivity to batchsize:

Figure 8 shows the performance comparison of different batch sizes taking values in the range of 20–80 (Car Hacking) and 1–20 (ROAD). It can be seen that too large or too small batch size will lead to the degradation of intrusion detection performance. The F1 score is highest when $B = 40$ (Car Hacking) and $B = 5$ (ROAD).

VI. DISCUSSION AND FUTURE WORK

According to the experimental results of performance observation of various methods under different window sizes, we can know that EfficientNet and MobileNetV3 perform well on ROAD dataset, while CANet performs well on Car Hacking dataset. However, their comprehensive performance on both datasets is weaker than StatGraph. This indicates that transforming CAN timing data into graph data interpretation may help to understand the internal features of the data and the use of multi-view graph and the selection of the appropriate perspective improve the generalization ability and refine identification granularity of the model. One of the benefits of fine granularity is that it allows for more effective traceability and defense. Attack source localization is possible when the granularity of identification for intrusion detection can be as detailed as identifying each message. Hence, designing a novel view graph that closely fits the interaction characteristics of

to overfitting. However, the small dimensionality of the latent

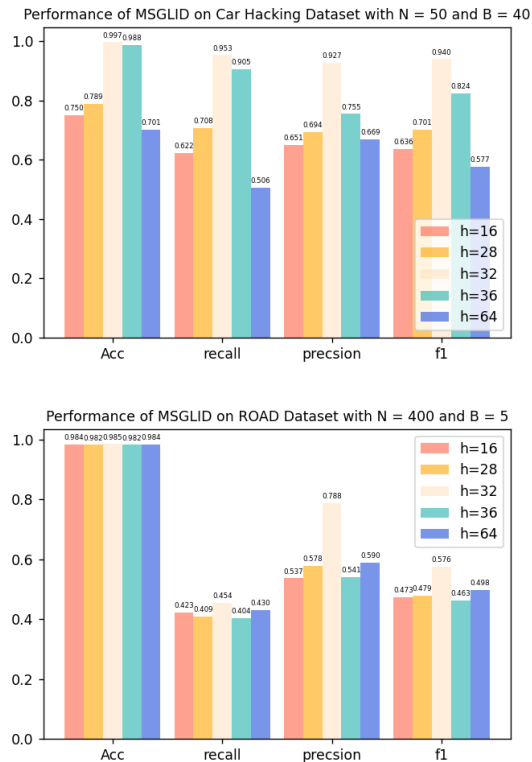


Fig. 7. Performance of StatGraph in Different Hidden-layer Units h .

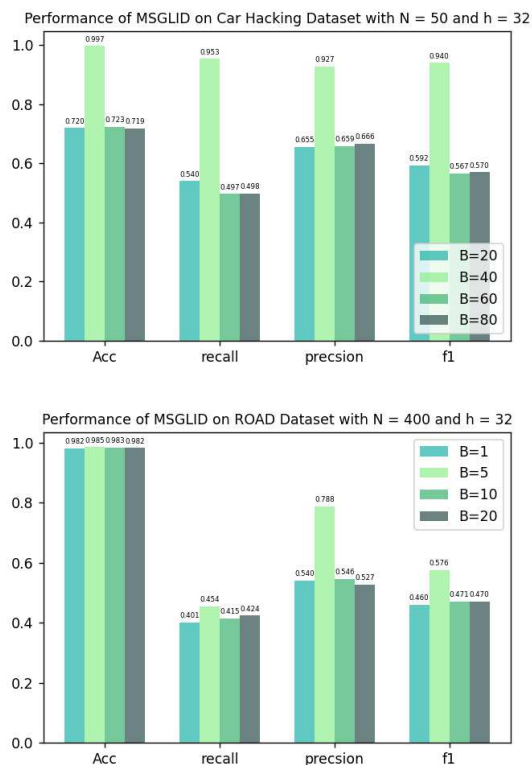


Fig. 8. Performance of StatGraph in Different Batchsize B .

ECUs is suggested for future research in the field of in-vehicle intrusion detection technology based on graph learning. Also we suggest adding traceability mapping module on message to source ECUs.

In addition, as a new dataset, the ROAD dataset certainly has the advantage of being true and diverse in terms of the types of masquerade attacks. However, one of the reasons for the failure of numerous intrusion detection approaches on the ROAD dataset is due to the fact that camouflage attacks are more stealthy. On the other hand, the lack or unbalance of samples in the dataset can also lead to less than optimal model learning. Therefore, through using data generation methods based on neural networks to solve the problem of sample imbalance and insufficient number of attack samples is also one of the future research directions of intrusion detection technologies.

VII. CONCLUSION

With the development and popularization of vehicle to everything communication, the increasing connectivity between vehicles and large networks makes it easier for attackers to hack through CAN to take over the vehicle. For the security of IVNs, intrusion detection methods based on deep learning have better performance than traditional manual feature extraction methods. However, these methods are too coarse-grained to protect CAN bus, for which we propose StatGraph which combines the advantages of the long-term statistical distribution feature of TCG and the short-term temporal correlation of CRG. The experiment result shows that StatGraph that combines two-view graphs and lightweight GCN implements efficient and fine-grained detection for each CAN message. In addition, we evaluate the performance of the classical convolutional neural network approach on ROAD dataset. In our future work, we will consider attack traceability based on fine-grained detection and investigate data generation models to address the problems of sample imbalance and less attack data.

REFERENCES

- [1] Hwanseok Harrison Jeong, Yiwen Chris Shen, Jaehoon Paul Jeong, and Tae Tom Oh. "A comprehensive survey on vehicular networking for safe and efficient driving in smart transportation: A focus on systems, protocols, and applications," in *Vehicular Communications*, 31:100349, 2021.
- [2] Sampath Rajapaksha, Harsha Kalutarage, M Omar Al-Kadri, Andrei Petrovski, Garikayi Madzudzo, and Madeline Cheah. Ai-based intrusion detection systems for in-vehicle networks: A survey. *ACM Computing Surveys*, 55(11):1C40, 2023.
- [3] Kai Wang, Hao Yin, Wei Quan, and Geyong Min. Enabling collaborative edge computing for software defined vehicular networks. *IEEE network*, 32(5):112C117, 2018.
- [4] Yong Xie, Gang Zeng, Ryo Kurachi, Fu Xiao, Hiroaki Takada, and Shiyun Hu. Timing analysis of can fd for security-aware automotive cyber-physical systems. *IEEE Transactions on Dependable and Secure Computing*, 2022.
- [5] Zhaojun Lu, Qian Wang, Xi Chen, Gang Qu, Yongqiang Lyu, and Zhenglin Liu. Leap: A lightweight encryption and authentication protocol for in-vehicle communications. In 2019 IEEE Intelligent Transportation Systems Conference (ITSC), pages 1158C1164. IEEE, 2019.
- [6] Kai Wang, Aiheng Zhang, Haoran Sun, and Bailing Wang. Analysis of recent deep-learning-based intrusion detection methods for in-vehicle network. *IEEE Transactions on Intelligent Transportation Systems*, 24(2):1843C1854, 2022.

- [7] Xiaokang Zhou, Wei Liang, Jinhua She, Zheng Yan, I Kevin, and Kai Wang. Two-layer federated learning with heterogeneous model aggregation for 6g supported internet of vehicles. *IEEE Transactions on Vehicular Technology*, 70(6):5308C5317, 2021.
- [8] Sampath Rajapaksha, Harsha Kalutarage, M Omar Al-Kadri, Andrei Petrovski, Garikayi Madzudzo, and Madeline Cheah. Ai-based intrusion detection systems for in-vehicle networks: A survey. *ACM Computing Surveys*, 55(11):1–40, 2023.
- [9] Hyun Min Song, Jiyoung Woo, and Huy Kang Kim. In-vehicle network intrusion detection using deep convolutional neural network. *Vehicular Communications*, 21:100198, 2020.
- [10] Miki E. Verma, Michael D. Iannacone, Robert A. Bridges, Samuel C. Hollifield, Pablo Moriano, Bill Kay, and Frank L. Combs. Addressing the lack of comparability & testing in can intrusion detection research: A comprehensive guide to can ids data & introduction of the road dataset. arXiv e-prints, 2020.
- [11] Siti-Farhana Lokman, Abu Talib Othman, and Muhammad-Husaini Abu-Bakar. Intrusion detection system for automotive controller area network (can) bus system: a review. *EURASIP Journal on Wireless Communications and Networking*, 2019:1–17, 2019.
- [12] Hongmao Qin, Mengru Yan, and Haojie Ji. Application of controller area network (can) bus anomaly detection based on time series prediction. *Vehicular Communications*, 27:100291, 2021.
- [13] Marcel Kneib and Christopher Huth. Scission: Signal characteristic based sender identification and intrusion detection in automotive networks. In *Proceedings of the 2018 ACM SIGSAC Conference on Computer and Communications Security*, pages 787C800, 2018.
- [14] R. Islam, Rud Refat, S. M. Yerram, and H. Malik. Graph-based intrusion detection system for controller area networks. *IEEE Transactions on Intelligent Transportation Systems*, PP(99):1C10, 2020.
- [15] Riadul Islam, Maloy K Devnath, Manar D Samad, and Syed Md Jaffrey Al Kadry. Ggnb: Graph-based gaussian naive bayes intrusion detection system for can bus. *Vehicular Communications*, 33:100442, 2022.
- [16] Valasek C and Miller C. Can message injection. *Black Hat USA*, p. 29, Jun, 2016.
- [17] T. N. Kipf and M. Welling. *Semi-supervised classification with graph convolutional networks*. 2016.
- [18] Hyunsung Lee, Seong Hoon Jeong, and Huy Kang Kim. Otds: A novel intrusion detection system for in-vehicle network by using remote frame. In *2017 15th Annual Conference on Privacy, Security and Trust (PST)*, pages 57C5709. IEEE, 2017.
- [19] Mee Lan Han, Byung Il Kwak, and Huy Kang Kim. Anomaly intrusion detection method for vehicular networks based on survival analysis. *Vehicular communications*, 14:52C63, 2018.
- [20] Eunbi Seo, Hyun Min Song, and Huy Kang Kim. Gids: Gan based intrusion detection system for in-vehicle network. In *2018 16th Annual Conference on Privacy, Security and Trust (PST)*, pages 1C6. IEEE, 2018.
- [21] Markus Hanselmann, Thilo Strauss, Katharina Dormann, and Holger Ulmer. Canet: An unsupervised intrusion detection system for high dimensional can bus data. *Ieee Access*, 8:58194C58205, 2020.
- [22] Du Hyun Min Song, and Huy Kang Kim. Automotive controller area network (can) bus intrusion dataset v2. [Online]. Available: <https://data.4tu.nl/repository/uuid:b74b4928-c377-4585-9432-2004dfa20a5d>, 2019.
- [23] Mingxing Tan and Quoc V. Le. Efficientnet: Rethinking model scaling for convolutional neural networks. 2019.
- [24] Andrew Howard, Mark Sandler, Grace Chu, Liang Chieh Chen, Bo Chen, Mingxing Tan, Weijun Wang, Yukun Zhu, Ruoming Pang, and Vijay Vasudevan. *Searching for mobilenetv3*. 2019.
- [25] Chi Zhang, Guosheng Lin, Fayao Liu, Rui Yao, and Chunhua Shen. Canet: Class-agnostic segmentation networks with iterative refinement and attentive few-shot learning. *IEEE*, 2019.
- [26] Miki E Verma, Robert A Bridges, Jordan J Sosnowski, Samuel C Hollifield, and Michael D Iannacone. Can-d: A modular four-step pipeline for comprehensively decoding controller area network data. *IEEE Transactions on Vehicular Technology*, 70(10):9685C9700, 2021.
- [27] Pawe Drodziel, Sawomir Tarkowski, Iwona Rybicka, and Rafa Wrona. Drivers reaction time research in the conditions in the real traffic. *Open Engineering*, 10(1):35C47, 2020.



Kai Wang received the B.S. and Ph.D. degrees from Beijing Jiaotong University. He is currently an Special Term Professor with the Faculty of Computing, Harbin Institute of Technology (HIT), China. Before joining HIT, he was a Post-Doctoral Researcher in computer science and technology with Tsinghua University. He has published more than 40 papers in prestigious international journals and conferences, including *IEEE Network*, *IEEE SYSTEMS JOURNAL*, *IEEE TRANSACTIONS ON NETWORK AND SERVICE MANAGEMENT*, and *ACM Transactions on Internet Technology*. His current research interests include lightweight and intelligent security technologies, such as deep learning applications on industrial control network or in-vehicle network intrusion detection. He is a Senior Member of the China Computer Federation (CCF).



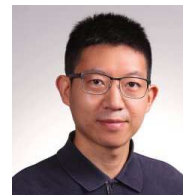
Qiguang Jiang received the B.S. degree in Information and Computing Science from the Harbin Institute of Technology (HIT), Weihai, China. She is currently pursuing the masters degree in computer science and technology with the Harbin Institute of Technology (HIT), China. Her research interests include intelligent and efficient in-vehicle intrusion detection models.



Bailing Wang received the Ph.D. degree from the School of Computer Science and Technology, Harbin Institute of Technology (HIT), China, in 2006. He is currently a Professor with the Faculty of Computing, HIT. He has published more than 80 papers in prestigious international journals and conferences, and has been selected for the China national talent plan. His research interests include information content security, industrial control network security, and V2X security.



Yongzheng Zhang is Chief Technology Officer (CTO) in the China Assets Cybersecurity Technology CO., Ltd. He respectively received the B.S. and Ph.D. degree from the Harbin Institute of Technology, China, in 2001 and 2006. Yongzheng Zhang was a full professor and Ph.D. supervisor in the Institute of Information Engineering, Chinese Academy of Sciences (CAS), China. His research interest includes network security. He has published more than 170 papers in refereed journals and conference proceedings. He was honored the first prize of Chinese National Award for Science and Technology Progress in 2011. He is a member of the IEEE. E-mail: zhangyz@cacts.cn



Yulei Wu is an Associate Professor working across the Faculty of Engineering and the Bristol Digital Futures Institute, University of Bristol, UK. He is also affiliated with the Smart Internet Lab and is a member of the High Performance Networks Research Group. He received his Ph.D. degree in Computing and Mathematics and B.Sc. (1st Class Hons.) degree in Computer Science from the University of Bradford, UK, in 2010 and 2006, respectively. His research interests focus on digital twins and ethics-responsible decision making and their applications on future networks, connected systems, edge computing, and digital infrastructure. Dr. Wu serves as an Associate Editor of *IEEE Transactions on Network and Service Management* (TNSM) and *IEEE Transactions on Network Science and Engineering* (TNSE), as well as an Editorial Board Member of *Computer Networks*, *Future Generation Computer Systems*, and *Nature Scientific Reports* at Nature Portfolio. He is chairing an IEEE Special Interest Group (SIG) on Ethical AI for Future Networks and Digital Infrastructure. He is a Senior Member of the IEEE and the ACM, and a Fellow of the HEA (Higher Education Academy).